Ground and Lowest-Lying Electronic States of CoN. A Multiconfigurational Study

João Paulo Gobbo and Antonio Carlos Borin*

Instituto de Química, Universidade de São Paulo Av. Prof. Lineu Prestes, 748 05508-900, São Paulo, SP, Brazil

Received: August 3, 2006; In Final Form: September 28, 2006

The lowest-lying $X^1\Sigma^+$, $a^3\Phi$, $b^3\Pi$, $c^5\Delta$, $A^1\Phi$, and $B^1\Pi$ electronic states of CoN have been investigated at the *ab initio* MRCI and MS-CASPT2 levels, with extended atomic basis sets and inclusion of scalar relativistic effects. Among the singlet states, the $A^1\Phi$ and $B^1\Pi$ states have been described for the first time. Potential energy curves, excitation energies, spectroscopic constants, and bonding character for all states are reported. Comparison with other early transition-metal nitrides (ScN, TiN, VN, and CrN), isoelectronic (NiC) and isovalent (RhN and IrN) species has been made, besides analyzing the $B^1\Pi \leftrightarrow X^1\Sigma^+$ electronic transition in terms of Franck−Condon factors, Einstein coefficients, and radiative lifetimes. At both levels of theory, the following energetic order has been obtained: $X^1\Sigma^+$, $a^3\Phi$, $b^3\Pi$, $c^5\Delta$, $A^1\Phi$, and $B^1\Pi$, with good agreement with experimental results. In contrast, previous DFT and MRCI calculations predicted the ground state to be the $^5\Delta$ state.

1. Introduction

Understanding the nature of the chemical bonding between transition metals and main group elements is fundamental in many fields, as for instance the interaction between transition metals and nitrogen atoms, which is a key step for a better understanding of the role of nitrogen fixation in both biological and industrial processes.[1,2] Nevertheless, very little is known about transition metal nitrides,[3] specially about the CoN species.

Andrews and co-workers[4,5] studied the reactions of laser-ablated Co atoms with nitrogen in argon at 10 K, concluding that CoN absorbs at 826.5 cm^{-1}; with the aid of density functional theory (DFT) calculations, they predicted that the CoN ground state would be a $^5\Delta$ state, with a low-lying $^3\Pi$ state 5 kcal/mol above it, followed by a $^1\Sigma^+$ excited state 6 kcal/mol above the putative $^5\Delta$ ground state. In some cases, DFT based methods can predict equilibrium properties fairly accurately;[6] however, according to Schaefer and co-workers[6] the accuracy is highly dependent upon the functional employed. In addition, DFT methods are not able to give a comprehensive view of several molecular electronic states.

Routine calculations on transition metal compounds are far from being trivial. The valence characteristics of the transition metal atoms give rise to a multitude of bonding schemes, from which several close-lying electronic states can be formed. For cobalt, for instance, the atomic configurations $3d^74s^2$ and $3d^8$-4s give rise to five LS atomic terms, with sixteen levels below 16 200 cm^{-1}.[7] Therefore, it is necessary to treat both nondynamic near-degeneracy problems and the strong dynamic correlation effects in a balanced matter, posing a great challenge to computational quantum chemistry.[3,8−10] During the last several years, we have described important aspects of NiC,[11,12] MnC,[13] and CoC,[14] employing high-level *ab initio* multiconfigurational methods, such as multireference configuration interaction (MRCI)[15−17] and multistate multiconfigurational second-order perturbation theory (MS-CASPT2)[8,18−20] methods, with which we can include the necessary correlation effects into the wave function.

On the basis of unpublished laser-induced fluorescence (LIF) spectra results that suggested that the ground state of CoN was $^1\Sigma^+$ in nature, Yamaki et al.[21] carried out MRCI calculations to identify the nature of the CoN ground state, employing Slater-type functions (Co, (9s7p5d2f1g); N, (7s5p2d1f)) augmented with diffuse and polarization functions. At the complete-active space self-consistent field (CASSCF) step, they included in the active space the Co 3d, 4s and N 2p orbitals and electrons, whereas at the MRCI step the active space was enlarged to include the N 2s2p orbitals and electrons as well. No relativistic effects were taken into account.

After exploratory calculations, Yamaki et al. focused on the $^5\Delta$,$^1\Sigma^+$, $^3\Phi$, and $^3\Pi$ electronic states, concluding that, at the MRCI level, the $^5\Delta$ should be the ground state, with the $^1\Sigma^+$ state located 0.183 eV above it. When higher-order excitations, estimated by a Davidson-type correction (MRSDCI+Q), were included, this scenario changed a little bit, with the $^1\Sigma^+$ state 0.116 eV above the $^5\Delta$ state. That is, the more electron correlation included, the closer the $^1\Sigma^+$ state is to the $^5\Delta$ state. To explore this aspect further, they carried out multireference coupled pair approximation (MRCPA) single point calculations at the $^1\Sigma^+$ and $^5\Delta$ equilibrium internuclear distances and concluded that the ground state would be the $^1\Sigma^+$ state, with the $^5\Delta$ state located 0.223 eV above it. Therefore, the potential energy curve for the CoN ground state still remains to be described. Furthermore, the nature of the low-lying excited states has not been investigated.

As implied above, the available results on CoN cannot be taken as conclusive. The potential energy curve for the ground state is still unknown; there are no data for the excited states and, consequently, for electronic transitions. On this basis, we have decided to investigate the lowest-lying electronic states of CoN at the MRCI and CASPT2 levels of theory with extensive basis sets, hoping to contribute to the chemical comprehension of this important species and inspiring future experimental work.

* Corresponding author. E-mail: ancborin@iq.usp.br. Fax: +55-11-3815 5579.

10.1021/jp065005i CCC: $33.50
Published on Web 12/21/2006

2. Methodology

The focus of this work is on the ground and lowest-lying electronic states of CoN. The Co ground state is ^{4}F ($3d^74s^2$)[7] with the following excited states (valence electron configuration and experimental excitation energies, averaged over the possible J values of each term, in parentheses): ^{4}F ($3d^8$ (^{3}F) 4s; 0.37 eV), ^{2}F ($3d^8$ (^{2}F) 4s; 0.82 eV), ^{4}P ($3d^74s^2$; 1.57 eV), and ^{4}P ($3d^8$ (^{3}P) 4s; 1.78 eV). The $2s^22p^3$ valence electron configuration is associated with the ground state of the N atom,[7] being represented by the ^{4}S° atomic term; the first excited state (^{2}D°, $2s^22p^3$) is located 2.38 eV above it. On the basis of these values, we concentrated on the low-lying molecular states that dissociate into the atomic ground states fragments, which combine[22] to form several molecular states of Σ^+, Π, Δ, and Φ spatial symmetry and multiplicity $(2S + 1) = 1$, 3, 5, and 7. Among them, the possible candidates for the ground state are $^5\Delta$, $^3\Pi$, and $^1\Sigma^+$.[3−5,21] For simplicity, in this work we have focused our attention on the lowest-lying $^1\Sigma^+$, $^{3,1}\Pi$, $^5\Delta$, and $^{3,1}\Phi$ molecular electronic states. It is interesting to note that the Co states ^{4}F ($3d^74s^2$, ground state) and ^{4}F ($3d^8$ (^{3}F) 4s, first excited state) have similar energies and that the radial extension of both 4s and 3d Co atomic orbitals are also similar. Therefore, the 4s and 3d Co orbitals may participate simultaneously in the bonding between the Co and N atoms.

Electron correlation (both dynamic and nondynamic) has been accounted for using two approaches. First, the MRCI method was employed, following the protocol used in our previous studies on NiC[11,12] and MnC.[13] The augmented triple-ζ atomic natural orbital (ANO) basis set of Roos and co-workers,[23] with the most diffuse g function removed from the set to keep the calculation feasible, was employed for describing the cobalt atom; it can be represented by the notation (21s15p10d6f4g)/[8s7p5d3f1g]. The nitrogen atom was described by spdf functions from the quadruple-ζ correlation-consistent basis set of Dunning and co-workers,[24−26] supplied with diffuse functions (aug-cc-pVQZ). As usual, only the spherical harmonic components of the basis functions were included in the calculations, amounting to a total of 146 contracted spherical Gaussian functions.

The MRCI calculations were carried out in two steps. Initially, the state-averaged complete-active-space self-consistent-field (SA-CASSCF)[15,16] method was employed to optimize the orbitals used in the one-particle space in the MRCI treatment, including in the active space the valence 3d and 4s Co orbitals and the 2s, 2p N orbitals. The calculations were carried out in the C_{2v} ($a_1b_1b_2a_2$) point group symmetry, with the atoms along the z-axis. With this orientation, the active atomic orbitals transform as $5a_1$ (Co 4s (σ), $3d_{x^2-y^2}$ ($d_{\delta+}$), $3d_{z^2}$ (d_σ)/N 2s (σ) and $2p_z$ (p_σ)), $2b_{1,2}$ (Co $3d_{xz,yz}$ (d_π)/N $2p_{x,y}$ ($2p_\pi$)), and $1a_2$ (Co $3d_{xy}$ ($d_{\delta-}$)), being represented as (5221). The averaging was carried out over the possible candidates for the ground state ($^5\Delta$, $^3\Pi$, and $^1\Sigma^+$ states) plus the $^3\Phi$ state, belonging to the A_1 ($^1\Sigma^+$), $B_{1,2}$ ($^3\Pi$,$^3\Phi$), and A_2 ($^5\Delta$), irreducible representations of the C_{2v} point group. It is worth mentioning that the $^3\Phi$ state was included in the averaging process, even though it is not a candidate for the ground state, because the $^3\Pi$ and $^3\Phi$ potential energy curves cross. All 590 $^5A_2$, 1308 $^1A_1$ and 1740 $^3B_{1,2}$ configuration state functions (CSFs), generated within the active space described above, were considered by us. Core 1s (Co, N) orbitals and the Co 2s, 2p, 3s and 3p semi-core orbitals were kept in the inactive space in all calculations.

Dynamic correlation effects were included in a second step, via the internally contracted multireference configuration interaction approach (ICMRCI),[27−30] with the reference space composed of the CSFs described above. All single and double excitations from the whole CASSCF active space were included in the final wave function, comprising a total of 71 940 069 $^5A_2$($^5\Delta$), 69 143 396 $^1A_1$($^1\Sigma^+$), 66 715 444 $^1B_1$($^1\Pi$), and 122 833 852 $^3B_1$($^3\Pi$,$^3\Phi$) CSFs, being further reduced 557 312 $^5A_2$, 846 056 $^1A_1$, 844 156 $^1B_1$ ($^1\Pi$) and 1 135 756 $^3B_{1,2}$ CSFs by employing the ICMRCI technique. The weight of the reference space was always larger than 80%. Relativistic corrections were taken into account through the Darwin contact and mass-velocity terms.[31,32] The CASSCF/ICMRCI calculations were performed using the MOLPRO-98.1 code.[33]

Potential energy curves (PEC) and the dipole transition moment function for the $B^1\Pi \leftrightarrow X^1\Sigma^+$ electronic transition were obtained by fitting cubic splines to the computed energies and dipole transition moments, from which vibrational wave functions, energies, spectroscopic constants and radiative lifetimes were obtained with the aid of the Vibrot[34] and Level 7.5[35] softwares, as done previously.[11−14,36] Rotationless Einstein coefficients for spontaneous emission ($A_{v'v''}$) for a particular vibronic transition were computed according to the expression proposed by Larsson.[37] Dissociation energy values, D_e, were computed using the supermolecule model, as the difference between the total energies of each electronic state at the equilibrium geometry and at an internuclear separation equal to 100.0 a_0.

The MS-CASPT2 approach[8,18−20] was the second alternative employed to treat correlation effects, following as close as possible the scheme used by us to investigate the electronic states of CoC.[14] The zeroth-order wave function was obtained by including the Co 3d and 4s orbitals and the N 2s and 2p orbitals in the active space; then, dynamic correlation effects were added using complete-active-space second-order perturbation theory (CASPT2) with the shifted zeroth-order Hamiltonian proposed by Ghigo, Roos, and Malmqvist,[38] with a shift parameter of 0.25 Hartree. During the MS-CASPT2 calculations, the Co 3s and 3p orbitals were also included in the active space; Co 1s, 2s, and 2p orbitals and the N 1s orbital were kept frozen. Intruder state problems were treated using an imaginary shift[39] of 0.1 Hartree; the Douglas−Kroll−Hess (DKH) approximation[40,41] was employed to take into account scalar relativistic effects. Quadruple-ζ atomic ANO-RCC[42] basis sets were employed for describing the atomic species, the Co atom being described by the uncontracted 21s15p10d6f4g2h set contracted to 7s6p4d3f2g and the N atom with the 14s9p4d3f primitive set contracted to 5s4p3d2f functions.[43]

The CASSCF/MS-CASPT2 calculations were carried out using the C_2 point group symmetry, on which the Σ^+ and Δ states belong to the first irreducible representation and the Π and Φ states belong to the second irreducible representation. Separate calculations were made for the states of different spin symmetry and orbital rotations were restricted to avoid mixing between different angular momenta. Therefore, at the CASSCF/MS-CASPT2 level, state specific calculations were carried out for the $X^1\Sigma^+$ and $c^5\Delta$ states, which means that the molecular orbitals were optimized separately for each of them. State-averaged calculations were carried out for describing the Π and Φ states (two Π and two Φ components) of each spin symmetry, because these states have components in the same irreducible representation. All components of the states belonging to the same irreducible representation and with the same spin were included in the multistate treatment at the CASPT2 level, with the aid of the MOLCAS-6.4[34] quantum chemistry software. Potential energy curves and spectroscopic constants were obtained as described above.

TABLE 1: Summary of Experimental and Theoretical Spectroscopic Constants for the Electronic States of the Molecule CoN[a]

state	T_e (kcal/mol)	R_e (Å)	D_e (eV)	ω_e (cm^{-1})	ref
$X^1\Sigma^{+a)}$		1.561[b]	1.97	914[b]	MRCI[c]
		1.573		888	MS-CASPT2[c]
		1.580	2.168	828	21[d]
		1.524		1089	5[e]
$a^3\Phi$	5.5	1.632	1.73	826	MRCI[c]
	8.3	1.613		927	MS-CASPT2[c]
	1.3		2.112		21[d]
$b^3\Pi$	6.5	1.618	1.69	862	MRCI[c]
	9.2	1.604		962	MS-CASPT2[c]
	0.8		2.132		21[d]
	−1	1.534		888	5[e]
$c^5\Delta$	8.4	1.604	1.61	862	MRCI[c]
	9.8	1.573		979	MS-CASPT2[c]
	−2.7	1.622	2.284	818	21[d]
	5.1				21[f]
	−6	1.588		859	5[e]
$A^1\Phi$	12.9	1.671	1.41	729	MRCI[c]
	11.7	1.626		837	MS-CASPT2[c]
$B^1\Pi$	19.6	1.630	1.12	670	MRCI[c]
	19.1	1.606		750	MS-CASPT2[c]

[a] All excitation energies were computed with the $X^1\Sigma^+$ state as the CoN ground state. [b] Experimental: $R_e = 1.575$ Å (see ref 21); $\omega_e = 826.5$ cm^{-1} (ref 21). [c] This work. [d] MRCI+Q. [e] DFT. [f] MRCPA.

TABLE 2: Vibrational Levels Spacings ($\Delta G_{v+1/2}$, in cm^{-1}) for the Lowest-Lying Quartet Electronic States of CoN

$\Delta G_{v+1/2}$	$X^1\Sigma^+$	$a^3\Phi$	$b^3\Pi$	$c^5\Delta$	$A^1\Phi$	$B^1\Pi$
0	904	820	857	860	727	674
1	889	810	846	852	720	675
2	877	800	838	837	715	673
3	867	791	829	836	709	669
4	858	777	819	826	699	664
5	845	757	805	813	683	655
6	826	735	785	798	664	641
7	808	716	764	776	647	625
8	797	697	743	755	630	608
$v = 0$	459	414	434	433	366	337

3. Results and Discussion

Computed spectroscopic constants and vibrational level spacings, respectively, for the $X^1\Sigma^+$, $a^3\Phi$, $b^3\Pi$, $c^5\Delta$, $A^1\Phi$, and $B^1\Pi$ electronic molecular states are reported in Tables 1 and 2. The corresponding potential energy curves are shown in Figure 1, the most relevant valence molecular orbitals (VMO) are plotted in Figure 2, and the $B^1\Pi \leftrightarrow X^1\Sigma^+$ dipole transition moment function is in Figure 3. Rotationless transition probabilities ($A_{v',v''}$), total Einstein coefficients ($A_{v'}$), radiative lifetimes ($\tau_{v'}$), obtained as the inverse of the total Einstein $A_{v'}$ coefficients for the lowest vibrational levels, Franck−Condon factors (FC), and excitation energies of various vibrational levels for the $B^1\Pi \rightarrow X^1\Sigma^+$ band system are displayed in Table 3.

3.1. Lowest-Lying $X^1\Sigma^+$, $a^3\Phi$, $b^3\Pi$, $c^5\Delta$, $A^1\Phi$, and $B^1\Pi$ Electronic States of CoN. Our MRCI calculation predicts that the ground state of CoN is a $X^1\Sigma^+$ state (see Table 1 and Figure 1), with an equilibrium internuclear distance (R_e) of 1.561 Å, dissociation energy (D_e) with respect to the Co (^{4}F ($3d^7\,4s^2$)) and N (^{4}S°($2s^2 2p^3$)) ground state atoms of 1.97 eV, and vibrational harmonic frequency (ω_e) of 914 cm^{-1}. These values can be compared with others published previously. The harmonic frequency obtained by Andrews and co-workers[5] in an argon matrix is 826.5 cm^{-1}, whereas the theoretical value obtained by density functional theory by the same authors is 1089 cm^{-1} ($R_e = 1.524$ Å). At the MRCI + Q level of theory, Yamaki et al.[21] obtained $R_e = 1.580$ Å, $\omega_e = 828$ cm^{-1}, and $D_e = 2.168$ eV. It is worth mentioning that neither the DFT calculations carried out by Andrews and co-workers nor the MRCI + Q of Yamaki et al. were able to identify the correct nature of the CoN ground state, which was identified as a $^5\Delta$ state in both cases. Nevertheless, after applying the MRCPA method to the equilibrium internuclear distance of the $^1\Sigma^+$ and $^5\Delta$ states, Yamaki et al. obtained the $^1\Sigma^+$ state 0.223 eV below the $^5\Delta$ state; on the basis of this finding, they identified the $^1\Sigma^+$ as being the CoN ground state. It is also interesting to note

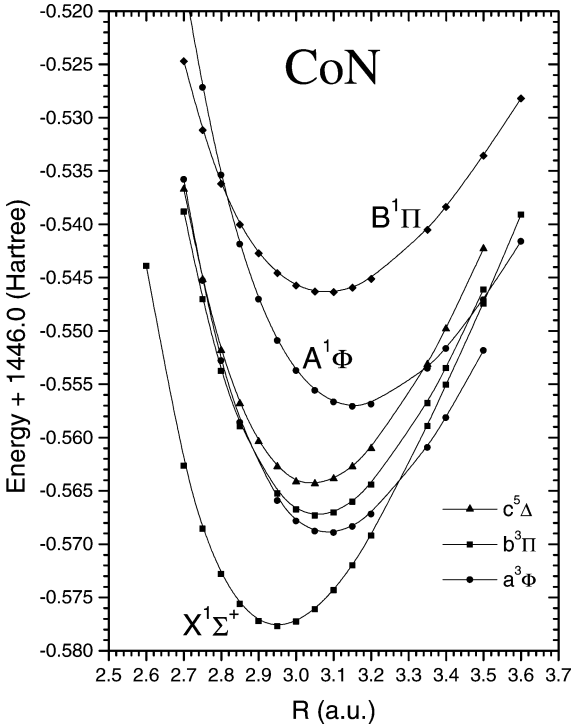

Figure 1. Potential energy curves for the lowest-lying singlet, triplet, and quintuplet electronic states of CoN.

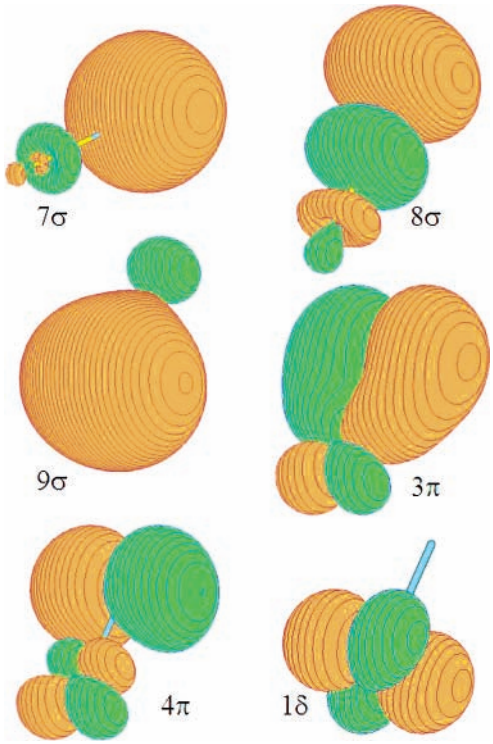

Figure 2. Valence molecular orbitals (VMO) involved in the chemical bonding between the Co and N atoms. The Co atom is the lower part of each VMO.

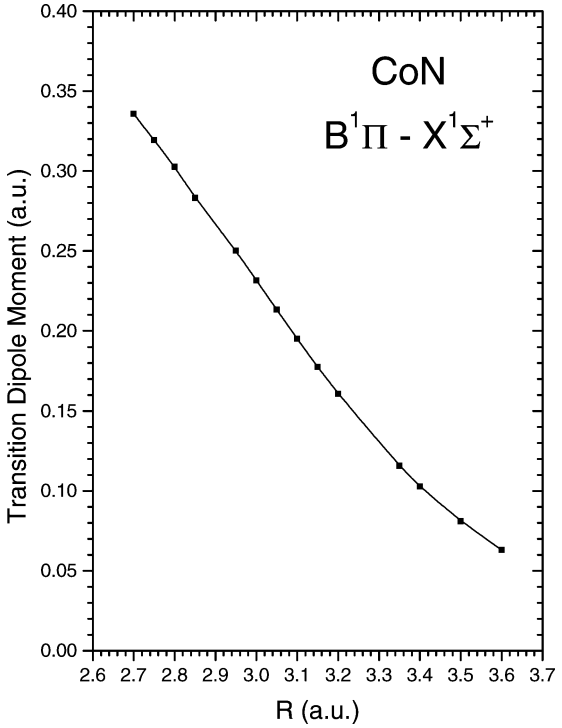

Figure 3. $B^1\Pi \leftrightarrow X^1\Sigma^+$ electronic transition dipole moment function of CoN.

that DFT methods can supply reliable results for equilibrium internuclear distances and harmonic frequencies, even when the nature of the ground state is wrong. In the case of transition metal mononitrides, the results reported in the literature indicate that DFT harmonic frequencies are higher than MRCI values,[3,5,44,45] except for TiN and VN, for which DFT and MRCI results are in agreement. As shown in Table 1, the results obtained at the MRCI and MS-CASPT2 levels are in good agreement, the MS-CASPT2 equilibrium internuclear distance being 0.012 Å larger and the vibrational frequency 26 cm^{-1} smaller than the corresponding MRCI values.

The $X^1\Sigma^+$ electronic ground state can be described mostly by a single electronic configuration:

$$|X^1\Sigma^+\rangle = (0.78)|...7\sigma^2 8\sigma^2 9\sigma^2 3\pi^4 1\delta^4\rangle + (0.27)|...7\sigma^2 8\sigma^2 9\sigma^2 3\pi^2 4\pi^2 1\delta^4\rangle$$

with the most important valence molecular orbitals (VMO), 7σ, 8σ, 9σ, 3π, and 1δ, being described around the ground state equilibrium internuclear distance (1.6 Å) as follows (see Figure 3). The 7σ is a nonbonding VMO corresponding to the 2s N atomic orbital. The 8σ VMO is a bonding orbital formed by the linear combination of the atomic $2p_z$ N orbital and a hybrid Co $4s3d_\sigma$ orbital; the 9σ VMO is the corresponding antibonding combination, polarized toward the Co atom. The 3π VMO is a bonding combination between the $3d_\pi$ ($3d_{xz}$ ($3d_{\pi x}$) and $3d_{yz}$ ($3d_{\pi y}$)) and $2p_\pi$ ($2p_x$ and $2p_y$) atomic orbitals from Co and N, respectively, distorted toward the N atom; the 4π VMO is the corresponding counterpart. Finally, the 1δ VMO orbital is, basically, an atomic orbital centered on cobalt, corresponding to the $3d_{x^2-y^2}$ ($3d_{\delta+}$) and $3d_{xy}$ ($3d_{\delta-}$) orbitals, attributing to it a nonbonding character. Therefore, the chemical bonding between the Co and N atoms in the $X^1\Sigma^+$ electronic ground state of CoN can be described by three normal electron-pair bonds (8σ and 3π VMO's) and three pairs of electrons localized on the Co atom (9σ and 1δ VMO's), plus one pair of electrons on the N atom (7σ VMO).

The nature of the chemical bonding between the Co and N atoms in the ground state of CoN can be compared with that of other early transition-metal nitrides, as for instance ScN, TiN, VN, and CrN.[46,47] In all these compounds, the ground state has a triple bond, with the remaining electrons localized on the transition metal. Comparisons can also be made with isoelectronic (for instance, NiC) and isovalent systems (for instance, RhN and IrN). As pointed out by us[11,12] and other authors,[48−50] the MRCI wave function for the $X^1\Sigma^+$ ground state of isoelectronic NiC species can be represented as 0.71 $|...7\sigma^2 8\sigma^2 9\sigma^2 3\pi^4 1\delta^4\rangle$ + 0.60$|...7\sigma^2 8\sigma^2 9\sigma^2 3\pi^3 4\pi^1 1\delta^4\rangle$, with an analogous interpretation for the VMO. Therefore, the ground state of NiC can also be described as having a triple bond, as in CoN. On the basis of the electron distribution derived from Mulliken population analysis, the occupancy of the 3d shell of Ni is intermediate between $3d^8$ and $3d^9$. At the CASSCF level, Shim, Mandix, and Gingerich[51] obtained a $^1\Sigma^+$ state as the ground state of RhN, which was further confirmed by other experimental and theoretical studies;[52−54] the major contribution to its CASSCF wave function is derived from the $|...10\sigma^2 11\sigma^2 12\sigma^2 5\pi^4 2\delta^4\rangle$ configuration, with the VMO's resembling the corresponding CoN ones. The chemical bonding has also been described as having a triple bond character, involving delocalized π and σ orbitals.[51] It is worth mentioning that the $^1\Sigma^+$ was obtained as the ground state of RhN only after including relativistic corrections at the CASSCF level[51] and that Citra and Andrews[53] could not predict the correct nature of the RhN ground state at the DFT level, as is the case for the CoN. The IrN molecule also has a $^1\Sigma^+$ ground state,[55−57] with the X state configuration as, in terms of valence atomic orbitals, $1\sigma^2 2\sigma^2 3\sigma^2 1\pi^4 1\delta^4$.[56,57] Again, the composition of the IrN valence molecular orbitals is very similar to that of the equivalent CoN valence molecular orbitals.

According to Harrison,[3] the triple bond could be formed from the Co ground state configuration ($^4F(3d^7 4s^2)$) or from the excited $^4P(3d^8 4s^1)$ configuration, with the $^4P(3d^8 4s^1)$ term dominating the CoN ground state molecular wave function, because the configuration $|\delta_+^2 \delta_-^2 \sigma \pi_x \pi_y\rangle$ is its major component (80%). Therefore, it is reasonable to suppose that the 3d population will be between eight (pure $^4P(3d^8 4s^1)$) and seven (pure $^4F(3d^7 4s^2)$), with the corresponding 4s population between one and two. The Mulliken population analysis for the X state (Co/N),

$$4s^{1.22} 4p_\sigma^{0.09} 3d_\sigma^{1.49} 3d_{\delta+}^{1.90} 3d_{\delta-}^{1.90} 3d_{\pi_x}^{1.03} 3d_{\pi_y}^{1.03} / 2s^{1.92} 2p_\sigma^{1.39} 2p_{\pi_x}^{0.97} 2p_{\pi_y}^{0.97}$$

indicates that the 3d and 4s Co shells are occupied by 7.35 and 1.22 electrons, respectively. This behavior is also observed for the ground state of NiC[11,50] and RhN. For RhN, it is interesting to remember that it not only dissociates into the atomic ground states ($^4F(4d^8 5s^1)$ + N ($^4S°(2s^2 2p^3)$) but also can be obtained by combining the nitrogen ground state atom and the Rh atom in either the $^4F(4d^8 5s^1$, ground) or $^2D(4d^9$, excited) states.[51]

Around its equilibrium internuclear distance (1.561 Å), the dipole moment of the $X^1\Sigma^+$ ground state is computed to be 2.37 D ($Co^{\delta+}N^{\delta-}$), which indicates that the CoN molecule is more polar than its isovalent species RhN, for which Shim et al.[51] reported a corresponding value of 2.08 D.

The lowest-lying electronic state of CoN (see Figure 1 and Table 1) is the $a^3\Phi$ state, lying 5.5 kcal/mol above the $X^1\Sigma^+$ ground state. With an equilibrium internuclear distance of 1.632 Å and ω_e = 826 cm^{-1}, the $a^3\Phi$ state dissociates to the ground atomic state (Co (^4F) + N ($^4S°$)) channel, with a corresponding

TABLE 3: Line Positions (LP, in cm^{-1}), Franck−Condon Factors ($q_{v'v''}$), Einstein Coefficients ($A_{v',v''}$, in s^{-1}), Total Einstein Coefficients ($A_{v'}$ in s^{-1}), and Radiative Lifetimes ($\tau_{v'}$, in μs) of Various Vibrational Levels v′of the B^{1}II State of CoN

v''/v'		$v'=0$	$v'=1$	$v'=2$	$v'=3$	$v'=4$	$v'=5$
0	LP	6747.25	7421.36	8096.27	8769.27	9439.61	10104.01
	$q_{v',v''}$	0.5471	0.3359	0.0979	0.0171	0.0018	0.0001
	$A_{v',v''}$	1.726(4)[a]	1.851(4)	9.202(3)	2.732(3)	5.161(2)	5.969(1)
1	LP	5843.10	6517.21	7192.12	7865.60	8535.46	9199.85
	$q_{v',v''}$	0.3228	0.0877	0.3308	0.1937	0.0548	0.0092
	$A_{v',v''}$	4.283(3)	2.457(3)	1.552(4)	1.547(4)	7.395(3)	2.148(3)
2	LP	4953.71	5627.82	6302.73	6976.21	7646.07	8310.46
	$q_{v',v''}$	0.1046	0.3055	0.0001	0.2109	0.2429	0.1059
	$A_{v',v''}$	5.483(2)	3.330(3)	1.192(0)	8.617(3)	1.667(4)	1.219(4)
3	LP	4076.76	4750.87	5425.78	6099.26	6769.12	7433.52
	$q_{v',v''}$	0.0220	0.1964	0.1927	0.0450	0.0910	0.2354
	$A_{v',v''}$	3.943(1)	8.280(2)	1.738(3)	6.509(2)	3.364(3)	1.399(4)
4	LP	3209.38	3883.49	4558.40	5231.88	5901.74	6566.13
	$q_{v',v''}$	0.0031	0.0616	0.2407	0.0862	0.1070	0.0194
	$A_{v',v''}$	1.580(0)	8.487(1)	8.179(2)	6.510(2)	1.396(3)	7.372(2)
5	LP	2351.42	3025.53	3700.44	4373.92	5043.78	5708.18
	$q_{v',v''}$	0.0003	0.0114	0.1087	0.2412	0.0210	0.1382
	$A_{v',v''}$	2.623(−2)	4.164(0)	1.160(2)	6.596(2)	1.374(2)	1.555(3)
6	LP	1504.95	2179.06	2853.97	3527.45	4197.31	4861.71
	$q_{v',v''}$	0.0001	0.0013	0.0255	0.1548	0.2125	0.0001
	$A_{v',v''}$	1.026(−4)	8.203(−2)	6.690(0)	1.283(2)	4.655(2)	1.604(0)
7	LP	674.21	1348.32	2023.23	2696.71	3366.57	4030.97
	$q_{v',v''}$	0.0000	0.0000	0.0033	0.0444	0.1927	0.1684
	$A_{v',v''}$	1.315(−6)	1.639(−4)	1.386(−1)	8.339(0)	1.234(2)	2.966(2)
8	LP					2549.26	3213.66
	$q_{v',v''}$					0.0654	0.2167
	$A_{v',v''}$					9.161(0)	1.089(2)
9	LP					1737.84	2402.24
	$q_{v',v''}$					0.0010	0.0883
	$A_{v',v''}$					1.653(−1)	9.144(0)
10	LP					932.85	1597.24
	$q_{v',v''}$					0.0008	0.0163
	$A_{v',v''}$					3.889(−4)	1.794(−1)
$Q_{v'}$		1.0000	0.9998	0.9997	0.9933	0.9909	0.9980
$A_{v'}$		22132.34	25215.28	27394.15	28920.14	30082.43	31097.57
$\tau_{v'}$		45.2	39.7	36.5	34.6	33.2	32.2

[a] Reads 1.726×10^4.

dissociation energy (D_e) of 1.73 eV; the dipole moment of the a$^3\Phi$ state is computed to be 2.77 D (Co$^{\delta+}$N$^{\delta-}$). Around its equilibrium internuclear distance, the a$^3\Phi$ MRCI wave function is described by the configuration

$$|a^3\Phi\rangle = (0.79)|...7\sigma^2 8\sigma^2 9\sigma^2 3\pi^4 4\pi^1 1\delta^3\rangle$$

which arises from the X$^1\Sigma^+$ ground state when one electron is excited from the occupied nonbonding 1δ VMO into the 4π antibonding VMO, represented by the single excitation (1$\delta \rightarrow$ 4π). This excitation results in an increase in the equilibrium internuclear distance and decreases the dissociation energy (R_e = 1.632 Å, D_e = 1.73 eV) in relation to that of its parent electronic state (R_e = 1.561 Å, D_e = 1.97 eV, for the X$^1\Sigma^+$ state). The Mulliken atomic distributions for the a$^3\Phi$ state can be described as (Co/N) $4s^{1.23}4p_\sigma^{0.09}3d_\sigma^{1.52}3d_{\delta+}^{1.44}3d_{\delta-}^{1.51}3d_{\pi_x}^{1.36}3d_{\pi_y}^{1.34}/2s^{1.91}2p_\sigma^{1.29}2p_{\pi_x}^{1.05}2p_{\pi_y}^{1.02}$. Overall, the a$^3\Phi$ state has three strong electron-pair bonds (8σ and 3π VMOs), one electron in an antibonding orbital (4π VMO), five electrons localized on Co atom, these being a pair of electrons in the 9σ VMO and three electrons on the 1δ ($3d_{x^2-y^2}$ and $3d_{xy}$ atomic orbitals) VMO, and one pair of electrons in the N atom (7σ VMO). It is worth mentioning that the MS-CASPT2 results (see Table 1) are in agreement with those obtained at the MRCI level, with the equilibrium internuclear distance 0.019 Å shorter, vibrational frequency 100 cm^{-1} higher, and excitation energy 3 kcal/mol higher than the values predicted at the MRCI level.

The MRCI calculations of Yamaki et al.[21] (see Table 1) placed the a$^3\Phi$ state 9.0 kcal/mol above the X state, whereas at the MRCI + Q level it is only 1.3 kcal/mol higher than the CoN ground state. A low-lying $^3\Phi$ state has also been found by us[12] for the isoelectronic NiC species (T_e = 30.6 kcal/mol, R_e = 1.748 Å, ω_e = 673 cm^{-1}, and D_e = 1.66 eV), it being the fourth excited state of NiC. As far as we know, there is no mention of a low-lying $^3\Phi$ state for RhN. On the other hand, the CASSCF/ICMRCI results for the isovalent IrN species, reported by Ram et al.,[57] show that there is a $^3\Phi$ state, described by an MRCI wave function dominated by the configuration (79%) $|...1\sigma^2 2\sigma^2 3\sigma^2 1\pi^4 2\pi^1 1\delta^3\rangle$, lying ($T_0$) 31.3 kcal/mol above the X state, with R_e = 1.700 Å and ω_e = 971 cm^{-1}, which makes it the second excited state of RhN.

The second excited state of CoN is the b$^3\Pi$ state (see Table 1), which also dissociates into the atomic ground state fragments (Co (^{4}F) + N (^{4}S°)), 6.5 kcal/mol (T_e) above the ground state. Its equilibrium internuclear distance is R_e = 1.618 Å, ω_e = 862 cm^{-1}, D_e = 1.69 eV, dipole moment of 2.78 D (Co$^{\delta+}$N$^{\delta-}$). As can be seen in Table 1, the MS-CASPT2 results follow the same trend observed for the $^3\Phi$ state; that is, the equilibrium internuclear distance is 0.014 Å shorter, the vibrational frequency 100 cm^{-1} higher, and the excitation energy 3 kcal/mol higher than the values predicted at the MRCI level.

The b$^3\Pi$ MRCI wave function, around its equilibrium internuclear distance, is similar to that for the a$^3\Phi$ state, but with different angular momenta coupling, its main configuration being

$$|b^3\Pi\rangle = (0.80)|...7\sigma^2 8\sigma^2 9\sigma^2 3\pi^4 4\pi^1 1\delta^3\rangle$$

which is derived from the $X^1\Sigma^+$ ground state by a single excitation ($1\delta \rightarrow 4\pi$), corresponding to a charge transfer from an atomic orbital centered on Co (1δ) to the antibonding 4π VMO. According to our results, the corresponding Mulliken population analysis is

$$4s^{1.23}4p_{\sigma}^{0.09}3d_{\sigma}^{1.51}3d_{\delta+}^{1.55}3d_{\delta-}^{1.45}3d_{\pi_x}^{1.33}3d_{\pi_y}^{1.33}/\\ 2s^{1.91}2p_{\sigma}^{1.27}2p_{\pi_x}^{1.03}2p_{\pi_y}^{1.07}$$

the chemical bonding in the $b^3\Pi$ state is similar to that described for the $a^3\Phi$.

The $b^3\Pi$ state was also investigated by Yamaki et al.[21] and Andrews and co-workers[5] (see Table 1). At the MRCI level with single and double excitations, Yamaki et al. located the $b^3\Pi$ state 8.8 kcal/mol above the X state. However, after estimating the influence of higher-order excitations employing a Davidson type quadruple excitation correction, they found the b state 0.8 kcal/mol above the X state. The DFT calculations carried out by Andrews and co-workers[5] placed the $b^3\Pi$ state 1 kcal/mol below the CoN $X^1\Sigma^+$ ground, at odds with previous MRCI results. For the isoelectronic species NiC, we have also found[12] a low-lying excited $^3\Pi$ state, 22.5 kcal/mol above the corresponding $X^1\Sigma^+$ ground state. Therefore, in CoN the manifold of excited states is much closer to the ground state than is predicted for NiC. In comparison to the isovalent RhN compound, a $^3\Pi$ state has also been found by Shim et al.[51] at the CASSCF level, with the inclusion of relativistic correction, as the lowest-lying electronic excited state, at 5.2 kcal/mol above the ground state and with an equilibrium internuclear distance of 1.676 Å, $\omega_e = 910$ cm^{-1}, and $D_e = 1.51$ eV. Around the equilibrium internuclear distance, the RhN $a^3\Pi$ state is best described by the configuration $|...10\sigma^2 11\sigma^2 12\sigma^1 5\pi^4 6\pi^1 2\delta^4\rangle$. The $^3\Pi$ state of RhN was observed experimentally in 1998[52] by anion photoelectron spectroscopy. As to the IrN isovalent species, Ram et al.,[57] with the aid of the CASSCF/ICMRCI methods and experimental absorption emission results recorded in the near-infrared region, determined that the lowest excited state is $a^3\Pi$ state, 22.9 kcal/mol above its ground state, with experimental ($R_e = 1.658$ Å and $\omega_e = 984$ cm^{-1}) and theoretical ($R_e = 1.673$ Å and $\omega_e = 1009$ cm^{-1}) spectroscopic constants in good agreement; around its equilibrium internuclear distance, the IrN $a^3\Pi$ state wave function can be described as (44%) $|...1\sigma^2 2\sigma^2 3\sigma^1 1\pi^4 2\pi^1 1\delta\rangle$ + (34%) $|...1\sigma 22\sigma^2 3\sigma^2 1\pi^4 2\pi^1 1\delta^3\rangle$.[57]

The next excited state is the $c^5\Delta$ state (Table 1), lying 8.4 kcal/mol above the ground state, with an equilibrium internuclear distance $R_e = 1.604$ Å vibrational constant $\omega_e = 862$ cm^{-1}, and dissociation energy with respect to the Co (^{4}F) + N (^{4}S°) ground state atomic fragment amounting to $D_e = 1.61$ eV; at the equilibrium distance, its computed dipole moment is 3.48 D ($Co^{\delta+}N^{\delta-}$). The main CSF's responsible for the MRCI wave function around its equilibrium configuration,

$$|c^5\Delta\rangle = (0.83)|...7\sigma^2 8\sigma^2 9\sigma^1 3\pi^4 4\pi^2 1\delta^3\rangle$$

is obtained from the X state by a double excitation (9σ, $1\delta \rightarrow 4\pi$), representing a charge transfer from the nonbonding 9σ and 1δ VMOs, located on the Co atom, to the antibonding 4π VMO localized on the C atom. Because one electron has been removed from a bonding VMO (9σ), the chemical bonding in the $c^5\Delta$ state is weaker than that for the $X^1\Sigma^+$ ground state, resulting in a decrease of the dissociation energy (from 1.96 to 1.61 eV, for the $X^1\Sigma^+$ and $c^5\Delta$ states, respectively) and an increase of the equilibrium internuclear distance (from 1.561 to 1.604 Å, respectively). The chemical bonding in the $c^5\Delta$ state is formed by three strong electron-pair bonds (8σ and 3π VMO's), two electrons in the antibonding 4π VMO, four electrons localized on the Co atom, one in the 9σ VMO and three in the 1δ ($3d_{x^2-y^2}$ and $3d_{xy}$ atomic orbitals) VMO, and one pair of electrons on the N atom (7σ VMO); the Mulliken population analysis is (Co/N): $4s^{0.89}4p_{\sigma}^{0.11}3d_{\sigma}^{1.18}3d_{\delta+}^{1.00}3d_{\delta-}^{1.96}3d_{\pi_x}^{1.58}3d_{\pi_y}^{1.58}/2s^{1.90}2p_{\sigma}^{0.97}2p_{\pi_x}^{1.24}2p_{\pi_y}^{1.24}$. Once more, the agreement among the MRCI and MS-CASPT2 results is good; the MS-CASPT2 equilibrium internuclear distance 0.031 Å shorter, the vibrational frequency 117 cm^{-1} higher, and the excitation energy 1.4 kcal/mol higher than the values predicted at the MRCI level.

The $c^5\Delta$ state was suggested to be the ground state by Andrews and co-workers;[5] on the basis of DFT calculations, they found the $c^5\Delta$ state to be 6 kcal/mol below the $X^1\Sigma^+$ state, with $R_e = 1.588$ Å and $\omega_e = 859$ cm^{-1}. In 2000, the MRCI calculations carried out by Yamaki et al.[21] placed it 4.2 kcal/mol below the $X^1\Sigma^+$ state; even at the MRCI + Q level, the $c^5\Delta$ state ($R_e = 1.622$ Å, $D_e = 2.284$ eV and $\omega_e = 818$ cm^{-1}) was found to be 2.7 kcal/mol below the $X^1\Sigma^+$ state. However, when single point MRCPA calculations were carried out at the MRCI + Q equilibrium distances for the $c^5\Delta$ and $X^1\Sigma^+$ states, the correct energetic order was obtained, with $c^5\Delta$ state located 5.1 kcal/mol above the $X^1\Sigma^+$ state. It is interesting to mention that, as the MRCPA T_e value was obtained by computing the total energies of the $X^1\Sigma^+$ and $c^5\Delta$ states at their MRCI + Q equilibrium internuclear distance, which may not correspond to the MRCPA equilibrium distances, the value reported by Yamaki et al. [21] must be taken as an estimate. Besides relativistic effects, not included in the MRCPA calculations by Yamaki et al.,[21] have a different influence on the $X^1\Sigma^+$ and $c^5\Delta$ states, stabilizing more the $X^1\Sigma^+$ state than the $c^5\Delta$ state;[21] therefore, after including the relativistic corrections, the T_e value should increase, as is indicated by our results. The results reported by us not only settle the correct energetic order but also supply reliable potential energy curves for the $X^1\Sigma^+$ and $c^5\Delta$ electronic states of CoN, which were not available previously. Comparison to the isoelectronic NiC and isovalent RhN and IrN cannot be made because the quintet states have not been investigated for these species.

The next two excited states included in our work are the $A^1\Phi$ and $B^1\Pi$ states. The $A^1\Phi$ has been found by us at 12.94 kcal/mol above the X state, with $R_e = 1.671$ Å, $\omega_e = 729$ cm^{-1}, dipole moment of 2.46 D ($Co^{\delta+}N^{\delta-}$), and $D_e = 1.41$ eV, in relation to its atomic dissociation channel (Co (^{4}F) + N (^{4}S°)). The leading configuration around its equilibrium internuclear distance is

$$|A^1\Delta\Phi\rangle = (0.74)|...7\sigma^2 8\sigma^2 9\sigma^2 3\pi^4 4\pi^1 1\delta^3\rangle$$

with the following Mulliken atomic distribution(Co/N):

$$4s^{1.24}4p_{\sigma}^{0.09}3d_{\sigma}^{1.40}3d_{\delta+}^{1.47}3d_{\delta-}^{1.49}3d_{\pi_x}^{1.44}3d_{\pi_y}^{1.43}/\\ 2s^{1.91}2p_{\sigma}^{1.39}2p_{\pi_x}^{0.97}2p_{\pi_y}^{0.97}$$

Therefore, relative to the $X^1\Sigma^+$ state, the $A^1\Phi$ state arises by promoting one electron from the 1δ to the 4π VMO, as observed for the $a^3\Phi$ state. For the isovalent NiC species, the $B^1\Phi$ state was found by us at 29.0 kcal/mol above the X state, which places it as the third excited state of NiC. To the best of our knowledge, no $^1\Phi$ state has been described for RhN. For IrN, however, the CASSCF/ICMRCI calculations carried out by Ram et al. [57] placed a $^1\Phi$ state 37 kcal/mol above the corresponding $X^1\Sigma^+$ ground state, characterizing it as the third excited state of IrN, dominated by a single configuration ((80%)$|...1\sigma^2 2\sigma^2 3\sigma^2 1\pi^4 2\pi^1 1\delta^3\rangle$).

The last electronic excited state of CoN included in this work is the $B^1\Pi$ state, lying 19.64 kcal/mol above the $X^1\Sigma^+$ ground state, with $R_e = 1.630$ Å, dipole moment of 2.66 D ($Co^{\delta+}N^{\delta-}$), and $\omega_e = 670$ cm^{-1}; its binding energy with respect to the lowest-lying ground state atomic channel (Co (^{4}F) + N (^{4}S°)) is 1.12 eV. In relation to its parent state ($X^1\Sigma^+$ ground state), the $B^1\Pi$ state is also characterized by a single-electron transfer from the 1δ VMO to the 4π VMO, with the main MRCI equilibrium configuration being described as

$$|B^1\Pi\rangle = (0.62)|...7\sigma^2 8\sigma^2 9\sigma^2 3\pi^4 4\pi^1 1\delta^3\rangle + (0.44)|...7\sigma^2 8\sigma^2 9\sigma^1 3\pi^4 4\pi^1 1\delta^4\rangle$$

The chemical bonding for the $A^1\Phi$ and $B^1\Pi$ states is similar to that described for the $a^3\Phi$ and $b^3\Pi$ states.

In comparison to other species, we have also identified an $^1\Pi$ excited state in NiC,[12] located 26.9 kcal/mol above the ground state, with $R_e = 1.773$ Å, $\omega_e = 539$ cm^{-1}, and $D_e = 1.82$ eV; it is the second lowest-lying excited state of NiC. RhN also exhibits a $^1\Pi$, which according to the CASSCF results of Shim et al. [51] is located 12.2 kcal/mol above the ground state, $R_e = 1.698$ Å and $\omega_e = 837$ cm^{-1}, being characterized as the second excited state of RhN. The existence of this state was confirmed experimentally by anion photoelectron spectroscopy[52] and gas-phase electronic spectroscopy[54] and found to be 11.2 kcal/mol above the X state. Several authors[55,58] have pointed out the existence of a $^1\Pi$ excited state in IrN, located around 15 200 cm^{-1} above its ground state; more recently, Bernarth and coauthors have found another $^1\Pi$ excited state 13 100 cm^{-1} above the ground state, which they have called the $A'^1\Pi$.

The MS-CASPT2 description of the $A^1\Phi$ and $B^1\Pi$ states is very similar to the one obtained at the MRCI level. The MS-CASPT2 equilibrium internuclear distances are 0.045 ($A^1\Phi$) and 0.024 Å ($B^1\Pi$) shorter, the vibrational frequencies are 108 and 80 cm^{-1} higher, for the $A^1\Phi$ and $B^1\Pi$ states, respectively, and the corresponding excitation energies 1.2 ($A^1\Phi$) and 0.5 kcal/mol ($B^1\Pi$) lower than the respective values obtained at the MRCI level.

3.2. $B^1\Pi \leftrightarrow X^1\Sigma^+$ Electronic Transition. Line positions (LP), Franck−Condon factors ($q_{v'v''}$), Einstein coefficients ($A_{v'v''}$), total Einstein coefficients ($A_{v'}$), and radiative lifetimes ($\tau_{v'}$) of various vibrational levels of the $B^1\Pi$ state of CoN are presented in Table 3 for the region between 1.4 Å ≤ R ≤ 1.9 Å, which corresponds to the Franck−Condon region. The behavior of the TDM function (Figure 3) can be analyzed by remembering the configurational nature of the $X^1\Sigma^+$ and $B^1\Pi$ states around the Franck−Condon region described. There are, basically, two excitations involved during the $B^1\Pi \leftrightarrow X^1\Sigma^+$ electronic transition; one corresponding to an excitation from the 1δ to the 4π VMO, and the other from the excitation from the 9σ to the 4π VMO. As discussed before, both the antibonding 9σ and nonbonding 1δ VMO's are centered on the Co atom, whereas the antibonding 4π VMO is centered on the N atom, indicating that, during the $B^1\Pi \leftrightarrow X^1\Sigma^+$ electronic transition, there is a charge transfer from the Co to the N atom. Therefore, in the Franck−Condon region, the electronic overlap integral between the most relevant molecular orbitals for describing the electronic transition decreases as the internuclear distance increases, which explains the behavior of the TDM in this region.

Based on the FC factors (Table 3), a general conclusion derived from the analysis of those data is that several vibrational levels of the $B^1\Pi$ state can be populated from the X state $v'' = 0$ vibrational level, with special emphasis on $v' = 0$ ($q_{0,0} = 0.5471$, 6747 cm^{-1}) and $v' = 1$ ($q_{1,0} = 0.3359$, 7421 cm^{-1}). In short, the most intense absorption bands originating from the $X^1\Sigma^+$ ($v'' = 0$) state are ($q_{v'v''}$): $q_{0,0} > q_{1,0} > q_{2,0} > q_{3,0}$; regardless of the initial vibrational level, the following sequence can be predicted: $q_{0,0}$(6747 cm^{-1}) > $q_{1,0}$(7421 cm^{-1}) > $q_{2,1}$(7192 cm^{-1}) > $q_{0,1}$(5843 cm^{-1}) > $q_{1,2}$(5628 cm^{-1}) > $q_{4,2}$(7646 cm^{-1}). Following this same semiquantitative reasoning based on the FC factors, we note that, during the emission process, the $X^1\Sigma^+$ ($v'' = 0$) vibrational level can be populated from $v' = 0-2$, in the following order: $q_{0,0} > q_{1,0} > q_{2,0}$.

The Einstein coefficients ($A_{v',v''}$) in Table 3 give a more quantitative analysis of the $B^1\Pi \leftrightarrow X^1\Sigma^+$ electronic transition. According to the relative intensities predicted by the $A_{v'v''}$ coefficients, the $X^1\sigma^+$ ($v' = 0$) vibronic level can be populated from $v' = 0-5$, with associated intensities corresponding to the following intensity order: $A_{1,0} > A_{0,0} > A_{2,0} > A_{3,0} > A_{4,0} > A_{5,0}$; this sequence differs from that based on FC factors indicated in the previous paragraph. As to the $X^1\Sigma^+$ ($v'' = 1$) vibrational level, the $A_{v',v''}$ coefficients suggest the following order for the emission process: $A_{2,1} \sim A_{3,1} > A_{4,1} > A_{0,1} > A_{1,1}$. The total radiative lifetime ($\tau_{v'}$) for the $X^1\Sigma^+$ ($v' = 0$) vibronic level is computed to be $\tau_0 = 45.2$ μs, becoming smaller as v' increases (39.7, 36.5, 34.6, and 33.2 μs) for $v' = 1 - 4$, respectively.

4. Conclusions

The lowest-lying $X^1\Sigma^+$, $a^3\Phi$, $b^3\Pi$, $c^5\Delta$, $A^1\Phi$, and $B^1\Pi$ electronic states of CoN have been investigated at the *ab initio* MRCI and MS-CASPT2 levels with extended atomic basis sets and inclusion of scalar relativistic effects. At the MS-CASPT2 level, the $3s^23p^6$ semicore correlation effects have also been taken into account. It is worth mentioning that our work is the first high-level multireference *ab initio* study of the $X^1\Sigma^+$, $a^3\Phi$, $b^3\Pi$, and $c^5\Delta$ states, with the $A^1\Phi$ and $B^1\Pi$ states being described for the first time. Potential energy curves, spectroscopic constants and dipole moments have been reported for all states. In contrast with previous DFT and MRCI results, we have identified the $X^1\Sigma^+$ state as the ground state of CoN at both levels of theory, with good agreement between the computed and experimental spectroscopic constants. At both levels of theory, the following energetic order has been obtained: $X^1\Sigma^+$, $a^3\Phi$, $b^3\Pi$, $c^5\Delta$, $A^1\Phi$, and $B^1\Pi$.

As to other early transition-metal nitrides (ScN, TiN, VN, and CrN), the chemical bonding in the $X^1\Sigma^+$ state has been described by three normal electron-pair bonds and three pairs of electrons localized on the Co atom plus one pair on the N atom; the same bonding scheme has also been found in the isoelectronic NiC as well as for isovalent RhN and IrN species. The most important VMOs, i.e., 7σ (a nonbonding VMO corresponding to the 2s N atomic orbital), 8σ (a bonding VMO formed by the linear combination of the atomic $2p_z$ N orbital and a hybrid Co $4s3d_\sigma$ orbital), 9σ (the corresponding antibonding combination, polarized toward the Co atom), 3π (a bonding combination between the $3d_\pi$ ($3d_{xz}$ ($3d\pi_x$) and $2p_x$ ($2p_y$) atomic orbitals from Co and N, respectively, distorted toward the N atom), 4π (the corresponding antibonding counterpart), and the 1δ VMO (a nonbondig orbital centered on cobalt, corresponding to the $3d_{x^2-y^2}$ ($3d_{\delta+}$) and $3d_{xy}$ ($3d_{\delta-}$) atomic orbitals), are also very similar to those found in ScN, TiN, VN, CrN, NiC, RhN, and IrN. Besides, the Mulliken population analysis indicates that the metal atom is positively charged, resulting in a dipole moment of 2.37 D.

The $B^1\Pi \leftrightarrow X^1\Sigma^+$ electronic transition has been also investigated for the first time, at the MRCI level, by means of FC factors, Einstein coefficients, and radiative lifetimes. The

Einstein coefficients indicate that the relative intensities of the emission band ending in the $X^1\Sigma^+$ ($v''= 0$) vibronic state are $A_{1,0} > A_{0,0} > A_{2,0} > A_{3,0} > A_{4,0} > A_{5,0}$. The total radiative lifetime ($\tau_{v'}$) for the $X^1\Sigma^+$ ($v' = 0$) vibronic level is computed to be $\tau_0 = 45.2\ \mu$s. A similar band system has also been reported in the literature for the NiC, RhN, and IrN species.

Acknowledgment. J.P.G. is grateful to FAPESP (Fundação de Amparo à Pesquisa do Estado de São Paulo, Brazil) for a graduate fellowship. A.C.B. acknowledges continuous academic support by the CNPq (Conselho Nacional de Desenvolvimento Científico and Tecnológico, Brazil) and FAPESP. We also thank the services and computer time of the Laboratório de Computação Científica Avançada (LCCA) of the Universidade de São Paulo.

References and Notes

(1) Leigh, G. J. *Science* **1998**, *279*, 506.
(2) Nishinayashi, Y.; Iwai, S.; Hidai, M. *Science* **1998**, *279*, 540.
(3) Harrison, J. F. *Chem. Rev.* **2000**, *100*, 679.
(4) Andrews, L. *J. Electron Spectrosc.* **1998**, *97*, 63.
(5) Andrews, L.; Citra, A.; Chertihin, G. V.; Bare, W. D.; Neurock, M. *J. Phys. Chem. A* **1998**, *102*, 2561.
(6) Barden, C. J.; Rienstra-Kiracofe, J. C.; Schaefer, H. F., III. *J. Chem. Phys.* **2000**, *113*, 690.
(7) Sansonetti, J.; Martin, W.; Young, S. *Handbook of Basic Atomic Spectroscopic Data (version 1.00)*; National Institute of Standards and Technology: Gaithersburg, MD, 2003; online available: http://physics-.nist.gov/Handbook.
(8) Roos, B. O.; Andersson, K.; Fülscher, M. P.; Malmqvist, P.-Å; Serrano-Andrés, L.; Pierloot, K.; Merchán, M. New Methods in Computational Quantum Mechanics. In *Advances in Chemical Physics*; Prigogine, I., Rice, S. A., Eds.; John Wiley & Sons: New York, 1996.
(9) Bauschlicher, C. W.; Langhoff, S. R.; Partridge, H. In *Modern Electronic Structure Theory*; Yarkony, D. R., Ed.; World Scientific: London, 1995.
(10) Partridge, H.; Langhoff, S. R.; Bauschlicher, C. W. In *Quantum Mechanical Electronic Structure with Chemical Accuracy*; Langhoff, S. R., Ed.; Kluwer Academic Publishers: Dordrecht: The Netherlands, 1995.
(11) Borin, A. C. *Chem. Phys.* **2001**, *274*, 99.
(12) Borin, A. C.; de Macedo, L. G. M. *Chem. Phys. Lett.* **2004**, *383*, 53.
(13) Borin, A. C.; Gobbo, J. P. *Chem. Phys. Lett.* **2006**, *417*, 334.
(14) Borin, A. C.; Gobbo, J. P.; Roos, B. O. *Chem. Phys. Lett.* **2006**, *418*, 311.
(15) Werner, H. J.; Knowles, P. J. *J. Chem. Phys.* **1985**, *82*, 5053.
(16) Knowles, P. J.; Werner, H. J. *Chem. Phys. Lett.* **1985**, *115*, 259.
(17) Roos, B. O. Ab Initio Methods in Quantum Chemistry - II. In *Advances in Chemical Physics*; Lawley, K. P., Ed.; John Wiley & Sons: Chichester, U.K., 1987.
(18) Andersson, K.; Malmqvist, P.-Å.; Roos, B. O.; Sadlej, A. J.; Wolinski, K. *J. Phys. Chem.* **1990**, *94*, 5483.
(19) Andersson, K.; Malmqvist, P.-Å.; Roos, B. O. *J. Chem. Phys.* **1992**, *96*, 1218.
(20) Finley, J.; Malmqvist, P.-Å.; Roos, B. O.; Serrano-Andrés, L. *Chem. Phys. Lett.* **1998**, *288*, 299.
(21) Yamaki, T.; Sekiya, M.; Tanaka, K. *Chem. Phys. Lett.* **2003**, *376*, 487.
(22) Herzberg, G. *Spectra of Diatomic Molecules*; Molecular Spectra and Molecular Structure Vol. I; Van Nostrand Reinhold: New York, 1950.
(23) Pou-Amerigo, R.; Merchán, M.; Nebot-Gil, I.; Widmark, P.-O.; Roos, B. O. *Theor. Chim. Acta* **1995**, *92*, 149.
(24) Dunning, T. H., Jr. *J. Chem. Phys.* **1989**, *90*, 1007.
(25) Dunning, T. H.; Harrison, R. J. *J. Chem. Phys.* **1992**, *96*, 6796.
(26) Woon, D. E.; Dunning, T. H. *J. Chem. Phys.* **1993**, *98*, 1358.
(27) Werner, H. J.; Knowles, P. J. *J. Chem. Phys.* **1988**, *89*, 5803.
(28) Knowles, P. J.; Werner, H. J. *Chem. Phys. Lett.* **1988**, *145*, 514.
(29) Werner, H. J. Ab Initio Methods in Quantum Chemistry - II. In *Advances in Chemical Physics*; Lawley, K. P., Ed.; John Wiley & Sons: Chichester, U.K., 1987.
(30) Werner, H. J.; Reinsch, E. A. *J. Chem. Phys.* **1982**, *76*, 3144.
(31) Cowan, R. D.; Griffin, D. C. *J. Opt. Soc. Am.* **1976**, *66*, 1010.
(32) Martin, R. L. *J. Chem. Phys.* **1983**, *87*, 750.
(33) Molpro (version 2000.1) is a package of *ab initio* programs written by Werner H.-J. and Knowles, P. J. with contributions from Almlöf, J.; Amos, R. D.; Berning, A.; Deegan, M. J. O.; Eckert, F.; Elbert, S. T.; Hampel, C.; Lindh, R.; Meyer, W.; Nicklass, A.; Peterson, K.; Pitzer, R.; Stone, A. J.; Taylor, P. R.; Mura, M. E.; Pulay, P.; Schuetz, M.; Stoll, H.; Thorsteinsson, T.; Copper. D. L.
(34) Karlström, G.; Lindh, R.; Malmqvist, P.-Å.; Roos, B. O.; Ryde, U.; Veryazov, V.; Widmark, P.-O.; Cossi, M.; Schimmelpfennig, B.; Neogrady, P.; Seijo, L. *Comput. Mater. Sci.* **2003**, *28*, 222.
(35) Le Roy, R. J. "Level 7.5 - A Computer Program for Solving the Radial Schrödinger Equation for Bound and Quasibound Levels", University of Waterloo, CP 655, 2002.
(36) Borin, A. C. *Chem. Phys. Lett.* **1996**, *262*, 80.
(37) Larsson, M. *Astron. Astrophys.* **1983**, *128*, 291.
(38) Ghigo, G.; Roos, B. O.; Malmqvist, P.-Å. *Chem. Phys. Lett.* **2004**, *396*, 142.
(39) Forsberg, N.; Malmqvist, P.-Å. *Chem. Phys. Lett.* **1997**, *274*, 196.
(40) Douglas, M.; Kroll, N. M. *Ann. Phys.* **1974**, *82*, 89.
(41) Hess, B. A. *Phys. Rev.* **1986**, *33*, 3742.
(42) Roos, B. O.; Lindh, R.; Malmqvist, P.-Å.; Veryazov, V.; Widmark, P.-O. *J. Phys. Chem. A* **2005**, *109*, 6575.
(43) Widmark, P.-O.; Malmqvist, P.-Å.; Roos, B. O. *Theor. Chim. Acta* **1990**, *77*, 291.
(44) Chertihin, G. V.; Andrews, L.; Bauschlicher, C. W., Jr. *J. Am. Chem. Soc.* **1998**, *120*, 3205.
(45) Andrews, L.; Bare, W. D.; Chertihin, G. V. *J. Phys. Chem. A* **1997**, *101*, 8417.
(46) Kunze, K. L.; Harrison, J. F. *J. Am. Chem. Soc.* **1990**, *112*, 3812.
(47) Harrison, J. F. *J. Phys. Chem.* **1996**, *100*, 3513.
(48) Kitaura, K.; Morokuma, K.; Csizmadia, I. G. *J. Mol. Struct. (THEOCHEM)* **1982**, *88*, 119.
(49) Shim, I.; Gingerich, K. A. *Z. Phys. D: Atoms, Molecules Clusters* **1989**, *12*, 373.
(50) Shim, I.; Gingerich, K. A. *Chem. Phys. Lett.* **1999**, *303*, 87.
(51) Shim, I.; Mandrix, K.; Gingerich, K. A. *J. Mol. Struc. (THEOCHEM)* **1997**, *393*, 127.
(52) Li, X.; Wang, L. *J. Chem. Phys.* **1998**, *109*, 5264.
(53) Citra, A.; Andrews, L. *J. Phys. Chem. A* **1999**, *103*, 3410.
(54) Fougère, S. G.; Balfour, W. J.; Cao, J.; Qian, C. X. W. *J. Mol. Spectrosc.* **2000**, *199*, 18.
(55) Steimle, T. C.; Marr, A. J.; Beaton, S. A.; Brown, J. M. *J. Chem. Phys.* **1997**, *106*, 2073.
(56) Ram, R. S.; Bernath, P. F. *J. Mol. Spectrosc.* **1999**, *193*, 363.
(57) Ram, R. S.; Liévin, J.; Bernath, P. F. *J. Mol. Spectrosc.* **1999**, *197*, 133.
(58) Marr, A. J.; Flores, M. E.; Steimle, T. C. *J. Phys. Chem.* **1996**, *104*, 8183.